RSC Advances

PAPER

View Article Online
View Journal | View Issue

Cite this: *RSC Adv.*, 2021, **11**, 33500

Self-assembly of the monohydroxy triterpenoid lupeol yielding nano-fibers, sheets and gel: environmental and drug delivery applications†

Saikat Kumar Panja, Soumen Patra and Braja Gopal Bag *

Lupeol is a medicinally important naturally abundant triterpenoid having a 6–6–6–6–5 fused pentacyclic backbone and one polar secondary "–OH" group at the C3 position of the "A" ring. It was extracted from the dried outer bark of *Bombax ceiba* and its self-assembly properties were investigated in different neat organic as well as aquous-organic binary liquid mixtures. The triterpenoid having only one polar "–OH" group and a rigid lipophilic backbone self-assembled in neat organic non-polar liquids like *n*-hexane, *n*-heptane, *n*-octane and polar liquids like DMSO, DMF, DMSO–H_2O, DMF–H_2O, and EtOH–H_2O yielding supramolecular gels *via* formation of nano to micrometre long self-assembled fibrillar networks (SAFINs). Morphological investigation of the self-assemblies was carried out by field emission scanning electron microscopy, high resolution transmission electron microscopy, atomic force microscopy, optical microscopy, concentration dependent FTIR and wide angle X-ray diffraction studies. The mechanical properties of the gels were studied by concentration dependent rheological studies in different solvents. The gels were capable of removing toxic micro-pollutants like rhodamine-B and 5,6-carboxyfluorescein as well as the toxic heavy metal Cr(VI) from contaminated water. Moreover release of the chemotherapeutic drug doxorubicin from a drug loaded gel in PBS buffer at pH 7.2 has also been demonstrated by spectrophotometry.

Received 13th August 2021
Accepted 1st October 2021

DOI: 10.1039/d1ra06137b

rsc.li/rsc-advances

1 Introduction

Terpenoids containing multiples of C5 units are a very large group of natural products present in plants as secondary metabolites. These are biosynthesized in plants from acetyl–CoA *via* a series of complex bio-chemical reactions in the presence of specific enzymes which produce diverse terpenoid structures containing hydroxyl and/or carboxyl groups in common.[1,2] The renewable and bio-compatible nature of plant derived terpenoids have made them significant in diversified areas of biological, chemical and materials science research.[3–5] Supramolecular terpenoid based gels obtained *via* hierarchical self-assembly have gained renewed interest in research for generating advanced renewable functional materials over the last two decades.[6–15] Gels based upon low molecular weight renewable chemicals have potential and realized applications in various research fields[16–19] like liquid crystals,[20] electro-conductive scaffolds,[21,22] sensing devices,[23] chemical catalysis,[24] nano-biotechnology, daily life applications,[6] advanced materials,[25] environmental remediation[26,27] *etc.* Physical as well as chemical gels[11,28–31] are typically obtained by self-assembly of low molecular weight components *via* non-covalent forces like H-bonding, electrostatic forces, dipole–dipole interactions, π–π interactions *etc.* The self-assembly properties of different types of amphiphilic molecules like long chain fatty acids,[32–34] sophorolipids,[35,36] peptides,[37–39] sugars,[40,41] and steroids,[42,43] have been explored extensively.

Since the first report of spontaneous self-assembly and gel formation of a naturally occurring terpenoid, different types of terpenoids have been explored for studying their self-assembly properties.[5,7,44,45] Tremendous biological and medicinal applications of lupeol like antiangiogenic,[46] anti-cancer,[47,48] anti-ulcer, hypoglycemic, anti-tumor,[49] antioxidant,[50] anti-inflammatory,[51] anti-bacterial,[52] antinociceptive effect,[53] hepatoprotective and antimicrobial activities have been reported.[54] Lupeol, a nano-sized terpenoid (1.35 nm) having both polar "–OH" group and lipophilic regions is an unique amphiphile for study of its self-assembly properties (Scheme 1). According to our knowledge, detailed self-assembly and gelation properties of lupeol in different liquids and their morphological characterizations have not yet been reported.[5–7,55] Herein, we report the self-assembly and gelation property of lupeol in different neat liquids as well as mixed liquids *via* formation of fibers, sheet having nano-to micro-meter dimensions. The morphology of gels of lupeol were characterized using several microscopic

Department of Chemistry and Chemical Technology, Vidyasagar University, Midnapore 721102, West Bengal, India

† Electronic supplementary information (ESI) available: Energy minimized structures, details of thermodynamic parameters, FTIR, rheology, mode of self-assembly based on crystal packing, microscopic images. See DOI: 10.1039/d1ra06137b

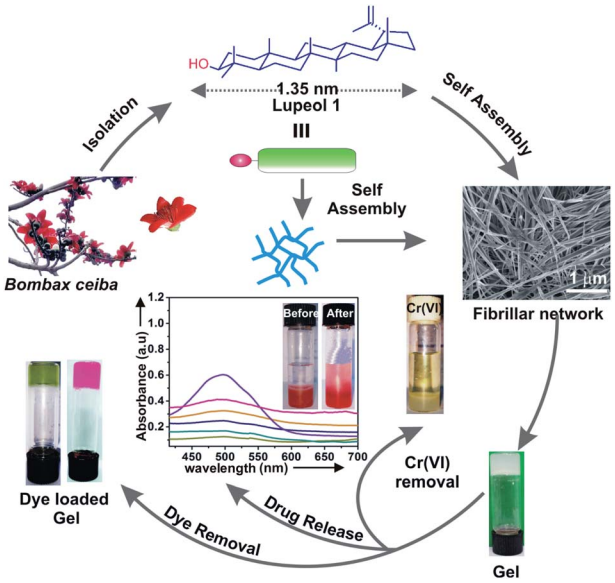

Scheme 1 Schematic presentation of isolation of lupeol **1** from *Bombax ceiba* and its self-assembly in liquids yielding gel *via* formation of fibrillar network and the various applications of gel.

techniques like optical microscopy (OPM), scanning electron microscopy (SEM), transmission electron microscopy (TEM), atomic force microscopy (AFM). Based on molecular modeling studies, X-ray diffraction data and FTIR studies, a model for the self-assembly of lupeol has also been proposed. Rheology of gels in different liquids at different concentrations have been carried out. Utilizations of the gel for toxic dye and heavy metal removal from contaminated water have been demonstrated. Moreover, release of anticancer drug doxorubicin from a drug loaded gel has been demonstrated using UV-visible spectrophotometry at physiological pH (pH = 7.2).

2 Results and discussion

2.1 Isolation of lupeol

We have isolated lupeol from the dried outer bark of indian flowering plant *Bombax ceiba* by following standard method developed in our laboratory and characterized by various spectroscopic techniques.[55] The purity of the sample used in this study was checked by ^{1}H and ^{13}C NMR, DEPT and HRMS.

2.2 Study of self-assembly properties

Lupeol **1** has a 6–6–6–6–5 fused pentacyclic lipophilic backbone attached with one hydroxy group at the 'A'-ring (C3 position). Energy minimization carried out by DFT calculation and by molecular mechanics calculation using Allinger's MMX algorithm revealed the length of the molecule as 1.35 nm (Fig. S1, and S2†). The large lipophilic moiety provided by the rigid pentacyclic backbone with the polar "–OH" group lying at the extreme end makes it an unique nano-sized amphiphile for the study of its self-assembly properties in liquids.

For studying the self-assembly property of lupeol, a weighed amount of the sample was dissolved in a liquid by heating (40–50 °C) for 20–25 min with magnetic stirring. The hot solution was kept at 15 °C under sealed condition for 2–8 h. When the vial was turned upside down, no flow of solvents indicated the formation of a gel. Gelation studies were carried out in 20 neat organic and aqueous-organic binary solvent mixtures. Lupeol spontaneously self-assembled to form gel in polar solvents like DMSO, DMF, DMSO–H_2O, DMF–H_2O and also in nonpolar solvents like *n*-hexane, *n*-heptane, *n*-octane *etc.* The T_{gel} values at their minimum gelator concentration were in the range 30–36 °C (Table 1). It was also observed that T_{gel} increased with increasing concentration of gelator which is reflected in their corresponding T_{gel} *vs.* concentration plots (Fig. 1 and S3, ESI†). All the gels obtained by self-assembly of lupeol were thermoreversible in nature as tested by repetitive heating and cooling experiments the sol-to-gel regained. A plot of ln *K vs.* $1/T_{gel}$ enabled us to calculate the various thermodynamic parameters

Table 1 Self-assembly studies of lupeol

Entry	Solvent	State[a]	MGC	T_{gel}[b] (°C)
1	DMSO	G	29.3	32
2	DMF	G	33.4	31
3	DMSO–H_2O (2 : 1 v/v)	G	25.5	36
4	DMSO–H_2O (3 : 2 v/v)	G	28.6	34
5	DMF–H_2O (2 : 1 v/v)	G	27.9	35
6	DMF–H_2O (3 : 2 v/v)	G	30.4	36
7	*n*-Hexane	G	39.1	32
8	*n*-Heptane	G	39.0	31
9	*n*-Octane	G	39.1	30
10	THF	VS	—	—
11	EtOH	VS	—	—
12	EtOH–H_2O (3 : 1 v/v)	VS	—	—
13	MeOH	VS	—	—
14	*n*-Butanol	VS	—	—
15	*n*-Hexanol	VS	—	—
16	*o*-Dichlorobenzene	VS	—	—
17	Mesitylene	VS	—	—
18	Nitrobenzene	VS	—	—
19	Cyclohexane	VS	—	—
20	Water	I	—	—

[a] G = gel, VS = viscous suspension, I = insoluble, minimum gelator concentration (MGC) are given in mM unit. [b] T_{gel} = gel to sol transition temperatures at MGCs.

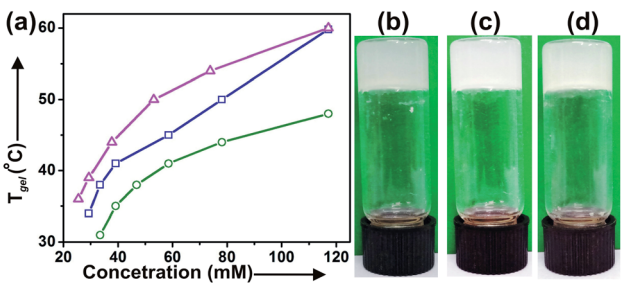

Fig. 1 (a) Plots of T_{gel} *vs.* concentration for **1** in DMSO–H_2O (2 : 1 v/v) (-▲-), DMSO (-■-), DMF (-●-). Gels of lupeol in (b) DMSO–H_2O (5.5% w/v, 128.9 Mm, 2 : 1 v/v), (c) DMSO (5% w/v, 117.3 mM), (d) DMF (5% w/v, 117.3 mM).

Table 2 Thermodynamic parameters (ΔH°, ΔS°, ΔG°) for gel to sol transition of gels of lupeol **1** in different liquids at 298 °K

Liquid	ΔH° kJ mol^{-1}	ΔS° J mol^{-1} K^{-1}	ΔG° kJ mol^{-1}
n-Hexane	82.0	242	10.0
n-Heptane	75.2	224	8.4
n-Octane	90.2	263	11.9
DMSO	54.6	179	9.7
DMF	69.8	199	10.5
DMSO–H_2O (2 : 1 v/v)	54.1	144	14.8
DMSO–H_2O (3 : 2 v/v)	47.1	123	13.4
DMF–H_2O (2 : 1 v/v)	48.4	126	13.8
DMF–H_2O (3 : 2 v/v)	48.0	124	13.8

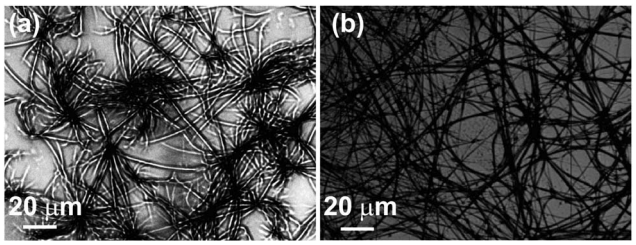

Fig. 2 OPM images of self assemblies of **1**: (a) in THF (2.5% w/v, 58.6 mM), (b) in *n*-heptane (2.5% w/v, 58.6 mM).

(ΔH°, ΔS°, ΔG°) at 298 K (Table 2 and Fig. S4, ESI†). The positive free energy changes (ΔG°) during gel to sol transformations in all the cases indicated the stability of the gels.

2.3 Morphological characteristics of the self-assemblies

The morphologies of the self-assemblies were studied by optical microscopy (OM), atomic force microscopy (AFM), field emission scanning electron microscopy (FESEM), and high resolution transmission electron microscopy (HRTEM).

2.3.1 Optical microscopic images. Optical microscopy (OM) was carried out in native state to investigate the microstructures of the self-assemblies of lupeol in various liquids. In THF (2.5% w/v, 58.6 mM) and *n*-heptane (2.5% w/v, 58.6 mM) optical microscopy revealed the formation of dense and entangled fibrillar network having fibers of several micrometers in length (Fig. 2a and b). OM was also carried out with the viscous suspensions of **1** in *n*-hexane (2% w/v, 46.9 mM), cyclohexane (1.5% w/v, 35.2 mM), *n*-heptane (1.5% w/v, 35.2 mM) and DMF–water (2% w/v, 46.9 mM, 1 : 1 v/v). In all these samples micrometer long fibrillar network were observed (Fig. S5, ESI†). Nano-fibers were not observed in OM due to the limitations of OM.

2.3.2 FESEM images. To further elucidate the self-assembled architectures, FESEM was carried out with the xerogels of **1** prepared from the viscous suspension of **1** in *n*-heptane (2% w/v, 46.9 mM), DMF (1.5% w/v, 35.2 mM) and EtOH (2% w/v, 46.9 mM). Xerogel of **1** in DMF revealed fibrillar network having thickness in the range 68–145 nm (Fig. 3d–f and S7a, b ESI†). Dried self-assemblies of **1** prepared from *n*-heptane revealed nano fibers having thickness 81–110 nm and several micrometer in length (Fig. 3a–c). FESEM of the xerogel of **1** prepared from ethanol (2% w/v, 46.9 mM) indicated the presence of fibrillar network (thickness 175–240 nm) (Fig. 4a–c) and sheet like morphologies (Fig. 4d–f and S7c, d ESI†).

2.3.3 Atomic force microscopic images. AFM was also carried out to investigate the morphologies of the xerogels of **1**. For this purpose, xerogels of **1** were prepared from a diluted colloidal suspension of **1** in neat organic liquid such as *n*-heptane (0.12% w/v, 2.8 mM), *o*-dichlorobenzene (0.11% w/v, 2.6 mM). Moreover, to elucidate the morphology of the self-assemblies in aqueous-organic binary liquid mixture dried

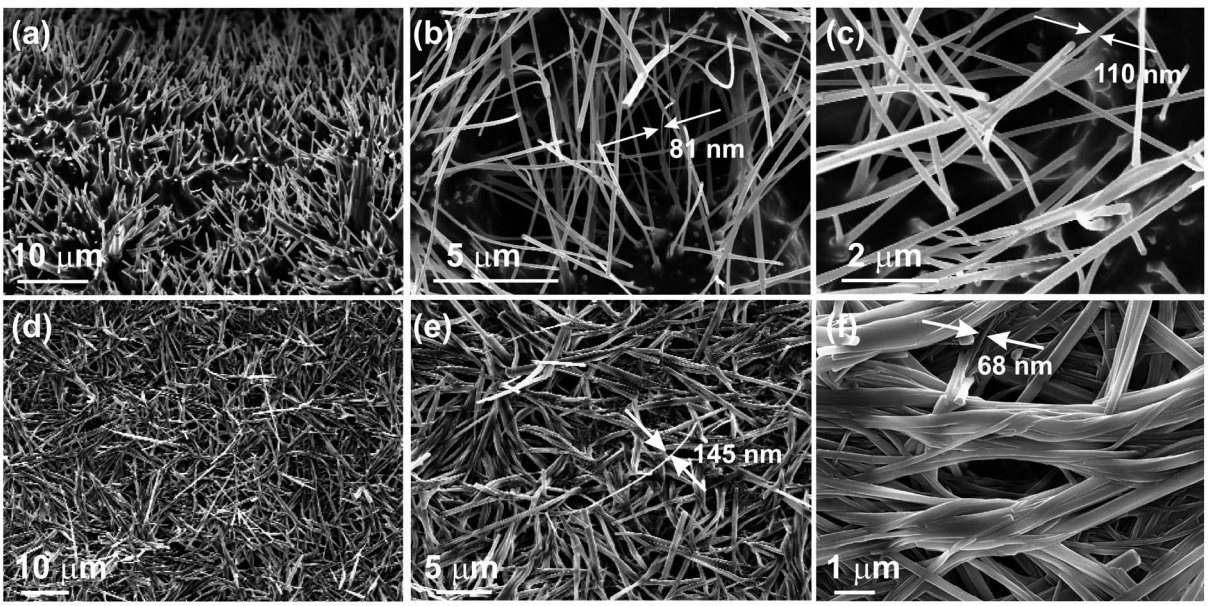

Fig. 3 FESEM micrographs of the dried self-assemblies of **1** prepared from (a–c) *n*-heptane (2% w/v, 46.9 mM), (d–f) DMF (1.5% w/v, 35.2 mM).

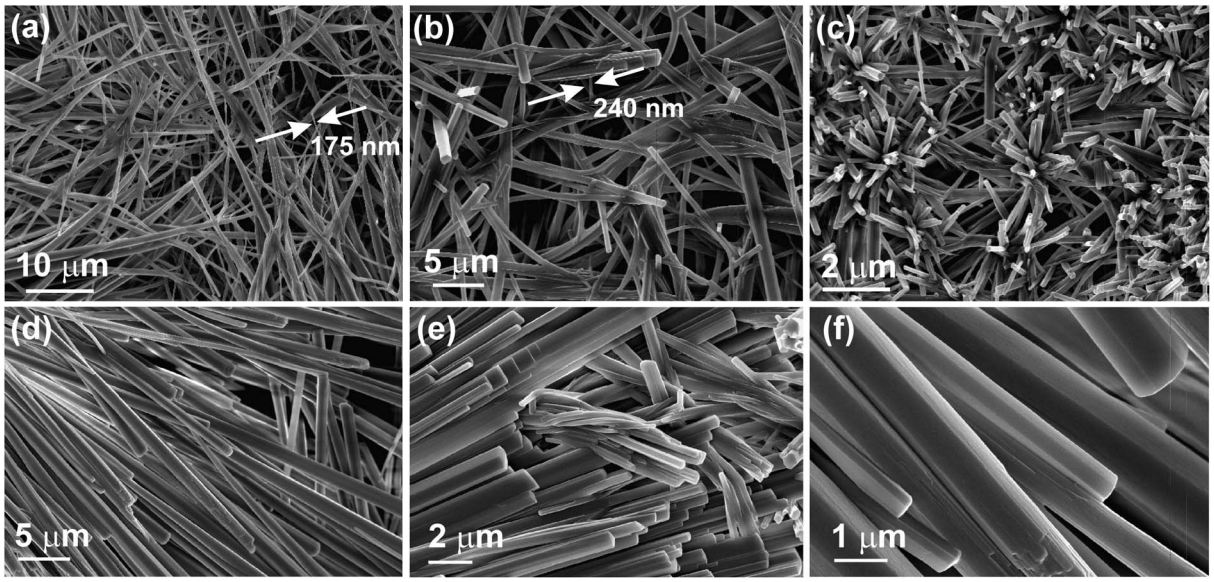

Fig. 4 FESEM micrographs of the dried self-assemblies of **1** prepared from (a–f) in EtOH (2% w/v, 46.9 mM).

sample was prepared from a diluted colloidal suspension of **1** in DMF–H_2O (1 : 1 v/v, 0.12% w/v, 2.8 mM) and AFM was carried out. Nano-to- micrometer thick fibrillar network and having length in micro-meter dimension were observed in all the xerogel samples studied (Fig. 5 and S6, ESI†).

2.3.4 HRTEM studies. To elucidate the self-assembled morphologies in further detail, we carried out HRTEM with the xerogels of **1** prepared from very dilute colloidal suspensions of **1** in THF (0.2% w/v, 4.7 mM) and *n*-heptane (0.13% w/v, 3.1 mM) (Fig. 6). TEM images obtained from the xerogel of **1** in THF (0.13% w/v, 3.1 mM) clearly indicated nano-fibers having thickness of 40–85 nm and length of nano to micrometer (Fig. 6a, b and d). Moreover, bundles of nano-fibers were also observed in the xerogel of **1** (Fig. 6c and S8, ESI†) prepared from *n*-heptane (0.2% w/v, 4.7 mM).

2.3.5 Rheology studies of the gels. Gels are soft, viscoelastic and semi-solid like materials. It exhibit both storage moduli (G') and dissipation of energy characterized by the loss moduli (G''). Rheology experiments enables one to understand various mechanical properties of the gels.[56–60] It was observed that with increasing strain/stress, G' and G'' moved parallel up to a certain point and after passing the linear region (LVER), a cross over between G' and G'' occurs. For a gel of **1** in DMSO–H_2O (2 : 1 v/v) at different concentrations (2.0% w/v (46.8 mM), 2.5% w/v (58.6 mM), 3.5% w/v (82.04 mM)) a cross over between G' and G''

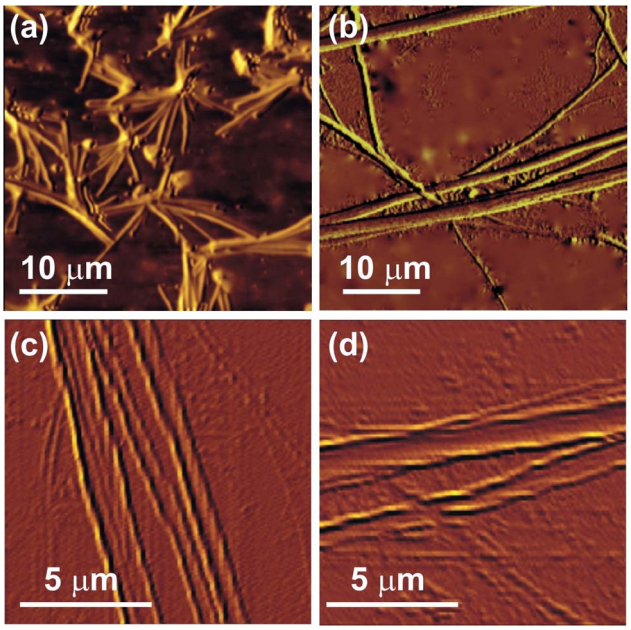

Fig. 5 AFM images of the dried self-assemblies of lupeol (a) in *n*-heptane (0.12% w/v, 3.5 mM), (b) in DMF–H_2O (0.12% w/v, 1 : 1 v/v, 2.8 mM), (c and d) in *o*-dichlorobenzene (0.11% w/v, 2.6 mM).

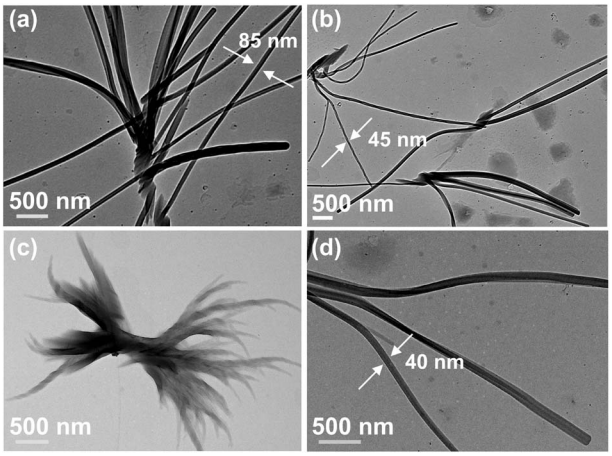

Fig. 6 Unstained HRTEM images of nano-fibers obtained from self-assemblies of lupeol (a, b and d) in THF (0.13% w/v, 3.1 mM), (c) bundle of nano-fibers in *n*-heptane (0.2% w/v, 4.7 mM).

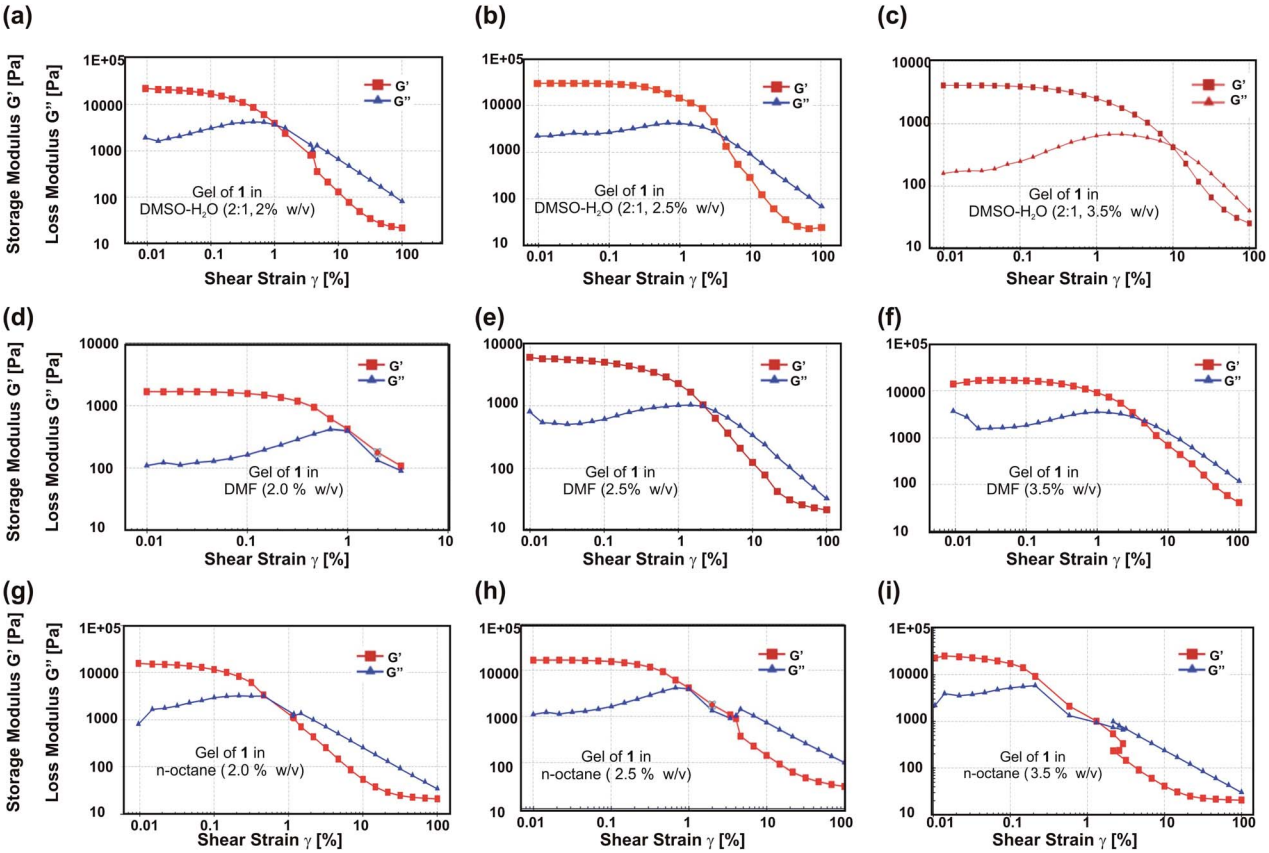

Fig. 7 Rheological studies of the gel of **1** (a–c) in DMSO–H_2O (2 : 1 v/v), (d–f) in DMF, (g–i) in *n*-octane at concentrations 2.0% w/v, 2.5% w/v and 3.5% w/v respectively.

occurred at critical strains (γ_c) 1.0%, 4.95% and 10.0% respectively (Fig. 7a–c). Similarly, for a gel of **1** in DMF at different concentrations (2.0% w/v, 2.5% w/v, 3.5% w/v) a cross over between G' and G'' occurred at a critical strain (γ_c) 1.0%, 3.2% and 4.95% respectively (Fig. 7d–f). For a gel of **1** in *n*-octane at different concentrations (2.0% w/v, 2.5% w/v, 3.5% w/v), a cross over between G' and G'' occurred at critical strains (γ_c) 0.46%, 1%, 2.1% respectively (Fig. 7g–i). From these experiments it was observed that with increasing the concentration of **1** in all the liquids tested, gel strength increased. This observation is consistent with our previous observations with concentration *vs.* gel-to-sol transition temperature (T_{gel}) plots (Fig. 1 and S3, ESI†). It was also observed that at an identical concentration mechanical strength of the gels are in order DMSO–H_2O (2 : 1 v/v) > DMF > *n*-octane. Thus with decreasing dielectric constant of the liquid, a decrease in gel strength was observed.[61,62] Moreover, it was also observed that all the gel samples tested were having high mechanical strength as the storage modulus (G') values for the gel is of the order of 10^3 to 10^5 Pa and $G' > G''$. The longer viscoelastic region (LVER) observed for all the gels in DMSO–water (2 : 1 v/v), DMF and *n*-octane, indicated that all the gels are viscoelastic in nature (Fig. 7, S10 and ESI†).

2.3.6 FTIR studies. Concentration dependent FTIR experiment was carried out to find out the driving force for the formation of the spontaneous self-assemblies and gelation properties of **1** *via* H-bonding in different liquids.[27,56,63,64] For this study, gels of **1** in both polar liquid like DMF and in non-polar liquid like *n*-heptane were prepared at different concentrations (0.6% w/v/14.06 mM, 1.5% w/v/35.16 mM, 3.0% w/v/70.32 mM). FTIR spectrum recorded for the neat compound **1**, the '–OH' stretching frequency appeared at 3312 cm^{-1} (Fig. 8). For samples prepared in DMF at concentrations 14.06 mM, 35.16 mM, and 70.32 mM, the stretching frequencies of '–OH' group appeared at 3310, 3307, 3279 cm^{-1} respectively (Fig. 8a). For the samples of **1** in *n*-heptane at similar concentrations (0.6% w/v, 1.5% w/v, 3.0% w/v) the '–OH' stretching frequencies

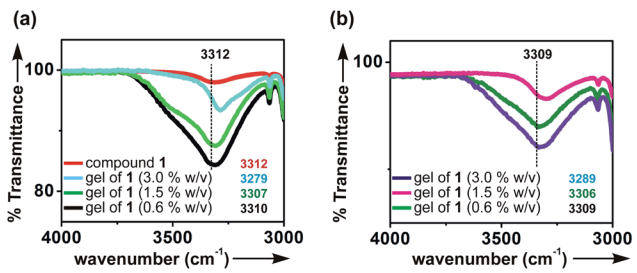

Fig. 8 Concentration dependent FTIR spectra of the gels of **1**: (a) in DMF, (b) in *n*-heptane. FTIR spectra are shown in the range 4000–3000 cm^{-1}. Concentration of the gels and the corresponding '–OH' stretching frequencies are shown using different colour.

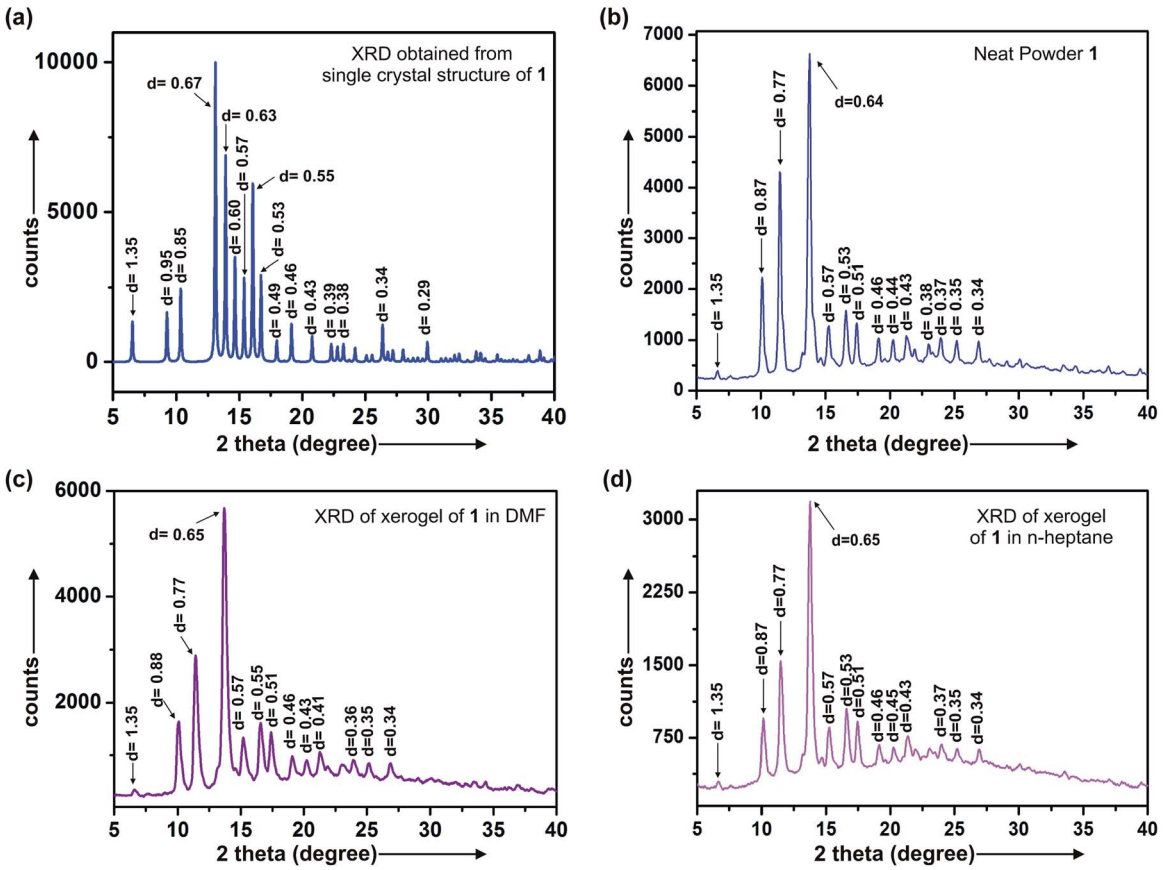

Fig. 9 X-ray diffractograms: (a) powder pattern generated from single crystal structure, (b) neat powder of **1**, (c) xerogel of **1** in DMF (2.5% w/v, 58.6 mM), (d) xerogel of **1** in *n*-heptane (2.5% w/v, 58.6 mM). *d*-spacing values are given in nm.

appeared at 3309, 3306, 3289 cm^{-1} respectively (Fig. 8b). It was observed that the stretching frequency of '–OH' group at 3312 cm^{-1} (compound **1**) shifted to 3279 cm^{-1} for the gel of **1** in DMF (70.32 mM) and to 3289 cm^{-1} for the gel of **1** in *n*-heptane (70.32 mM) respectively. Comparing the data, it is evident that irrespective of the nature of the liquids (polar/nonpolar), stretching frequencies of '–OH' group decreased along with peak broadening with increasing concentrations of **1** in the liquids tested. Comparing the FTIR spectral data, it was also observed that at an identical concentration (70.32 mM), the stretching frequency of '–OH' group decreases more in polar liquid like DMF compared to nonpolar liquid like *n*-heptane (Fig. 8a and b). From, these observations it is evident that gel formation *via* self-assembly of compound **1** is better in polar liquid compared to non-polar liquid. These observations are consistent with T_{gel} (Fig. 1 and S3, ESI†) and rheology data (Fig. 7, S10, ESI†) discussed earlier. All these observations also clearly indicate the significant role of H-bonding (between the '–OH' groups) interactions in gel formation *via* self-assembly of **1**. Moreover, the higher '–OH' stretching frequencies observed for the xerogels of **1** prepared from gels/viscous suspensions in *n*-hexane, *n*-octane, THF, *o*-dichlorobenzene and *n*-butanol at 3306, 3304, 3298, 3307, 3304 cm^{-1} respectively also support the observations by FTIR that during self-assembly and gelation lowering of the O–H stretching frequencies take place (Fig. S11, ESI†).

Table 3 XRD studies

Entry	*d* (nm)
Neat powder of **1**	1.35, 0.87, 0.77, 0.64, 0.57, 0.53, 0.51, 0.46, 0.44, 0.42, 0.39, 0.38, 0.35, 0.34, 0.30, 0.28, 0.27
XRD from single crystal	1.35, 0.95, 0.85, 0.67, 0.63, 0.60, 0.57, 0.55, 0.53, 0.49, 0.46, 0.43, 0.39, 0.38, 0.37, 0.34, 0.32, 0.31, 0.29
Xerogel in DMF	1.35, 0.88, 0.77, 0.65, 0.57, 0.55, 0.51, 0.46, 0.43, 0.40, 0.36, 0.33
Xerogel in *n*-heptane	1.35, 0.87, 0.77, 0.65, 0.57, 0.53, 0.51, 0.46, 0.45, 0.44, 0.37, 0.35, 0.34, 0.28

2.3.7 X-ray diffraction. Powder X-ray diffraction studies help to understand the nature of the self-assemblies. Wide angle powder XRD studies were carried out at 2θ (degree) = 5–40° with the neat powder of lupeol and xerogels prepared from gel samples in *n*-heptane (2.5% w/v, 58.6 mM) and DMF (2.5% w/v, 58.6 mM) (Fig. 9 and Table 3). Peaks obtained from both the xerogels and the neat powder of **1** were compared with the powder X-ray diffraction pattern generated from its single crystal structure (Fig. 9 and Table 3).[69]

The length of the molecule obtained by energy minimization as well as by X-ray crystallography is 1.35 nm. The 1.35 nm peak was common in all the diffraction data. XRD peaks observed at 1.35, 0.65, 0.46 nm for both the xerogels prepared from the gels in DMF and *n*-heptane are close to the ratio 1 : 1/2 : 1/3 indicating a lamellar pattern of self-assembled microstructures like fibrillar network/crystalline fibers, sheets which are consistent with our microscopic observations by SEM, HRTEM, AFM discussed earlier.[65–67]

A few peaks at 0.57, 0.46, 0.43, 0.34 nm found in the powder diffraction pattern generated from its single crystal structure were also observed in the xerogels of **1** from *n*-heptane and DMF as well as the neat powder indicating that ordered arrangement of molecules are also present in the gel morphology. The peaks at 0.95, 0.85, 0.67, 0.63, 0.60, 0.49, 0.39 nm observed in the single crystal did not match with the diffraction pattern from the xerogels of **1** in DMF and *n*-heptane indicating the uniqueness of the gel morphologies different from the single crystal (Fig. 9a–c and Table 3).

The 0.88, 0.77, 0.51, 0.36 nm peaks observed from DMF xerogel and 0.87, 0.77, 0.51, 0.37 nm peaks observed from the xerogel of **1** in *n*-heptane had several common or very close peaks with the diffraction pattern of neat powder 0.87, 0.77, 0.51, 0.42, 0.39, 0.30 nm also supports the uniqueness of gel morphology (Fig. 9a–d and Table 3).

2.3.8 Proposed model for molecular self assembly. Based on the observations from FTIR studies, powder X-ray diffraction studies, thorough inspection of the packing of the molecules in the crystal structure of **1**,[68] and molecular modelling studies, various possible modes for the formation of the self-assemblies of **1** has been proposed (Fig. 10 and S12–S16, ESI†). The molecule having the nano-metric length 1.35 nm and the presence of unsymmetrical terpenoids moiety gives rise two non-identical lipophilic surfaces such as α and β faces. This unsymmetrical nature of the lipophilic surfaces gives rise to various modes of stacked arrangements such as parallel ββ/αα and anti-parallel stacked arrangements αβ/βα.[69] The polar –OH group present at C3 position of lupeol also participate in intermolecular H-bonding as evident from FTIR studies. All of these interactions facilitate the spontaneous self-assembly of mono-hydroxy triterpenoid lupeol to form gel *via* formation of various nano-to micro sized self-assembled structures like fibrillar network, sheet.

3 Utilization of gel

3.1 Removal of toxic dyes from water

Gels are the semisolid-like materials having three dimensional fibrillar network inside, posses high surface area. The surface of the fibrillar network inside the gel moiety was utilized for studying the removal of toxic pigments such as rhodamine-B, CF from their respective aqueous solutions. For studying the removal of toxic dye rhodamine-B from its aqueous solution by

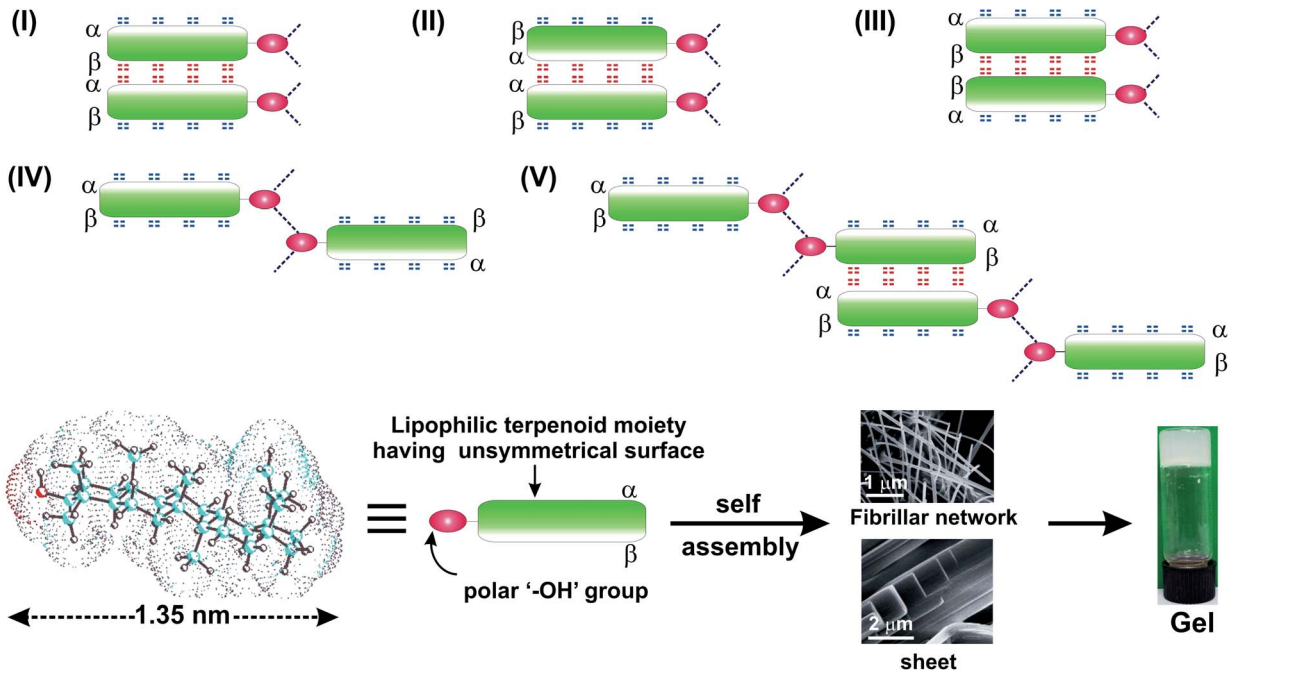

Fig. 10 Schematic presentation of possible modes of self-assembly of **1** yielding fibrillar network and gel. The '–OH' group can take part in H-bonding and the lipophilic terpenoids moiety can interact *via* van der Waals interaction. The unsymmetrical surfaces α and β of the terpenoids moiety leads to various types of assembly (I–V).

the gel, aqueous solution of rhodamine-B (0.2 mM, 1.5 mL) was prepared. Then the freshly prepared aqueous solution of dye was placed on the gel surface carefully. The removal of dye from its aqueous solution was monitored by UV-visible spectrophotometry. For the removal of anionic 5,6-carboxyfluorescein (CF), aqueous solution of CF (0.2 mM, 1.5 mL) was prepared and similar experiment was carried out. With increasing the time decreasing trend of absorption for both the cases observed, clearly indicated removal of dyes from their respective aqueous solution (Fig. 11a and b). Removal of toxic dyes from water *via* adsorption by the fibrillar network inside the gels were also confirmed by epifluorescence microscopy images as bright green and red fluorescence lights were observed after the adsorption of fluorophores (Fig. S9, ESI†).

3.2 Removal of heavy metal Cr(VI) from contaminated water

For studying the removal of toxic heavy metal Cr(VI), 0.05 mM (1.5 mL) aqueous solution of Cr(VI) was prepared freshly. A gel was prepared by dissolving 8 mg of **1** in DMSO–water (20.8 mM, 2 : 1 v/v). Then the freshly prepared aqueous solution of Cr(VI) was placed on the gel surface carefully. The removal of Cr(VI) from its aqueous solution was monitored by UV spectrophotometry. For this an aliquot of aqueous solution containing Cr(VI) was collected from the gel surface and absorption was measured at different time interval. With the increase in time decreasing trend of absorbance was observed which clearly indicated the removal of heavy metal from contaminated water by the gel (Fig. 11c).

3.3 Application of gel for release of anticancer drug doxorubicin in PBS buffer from loaded gel

A coloured gel of **1** in DMSO–water (3 : 2 v/v) loaded with anticancer drug doxorubicin (0.15 mM) was prepared. For the release of doxorubicin from the drug loaded gel into PBS buffer (pH 7.2), the buffer solution was placed carefully on the gel. Increase of the absorbance values of the buffer layer with time

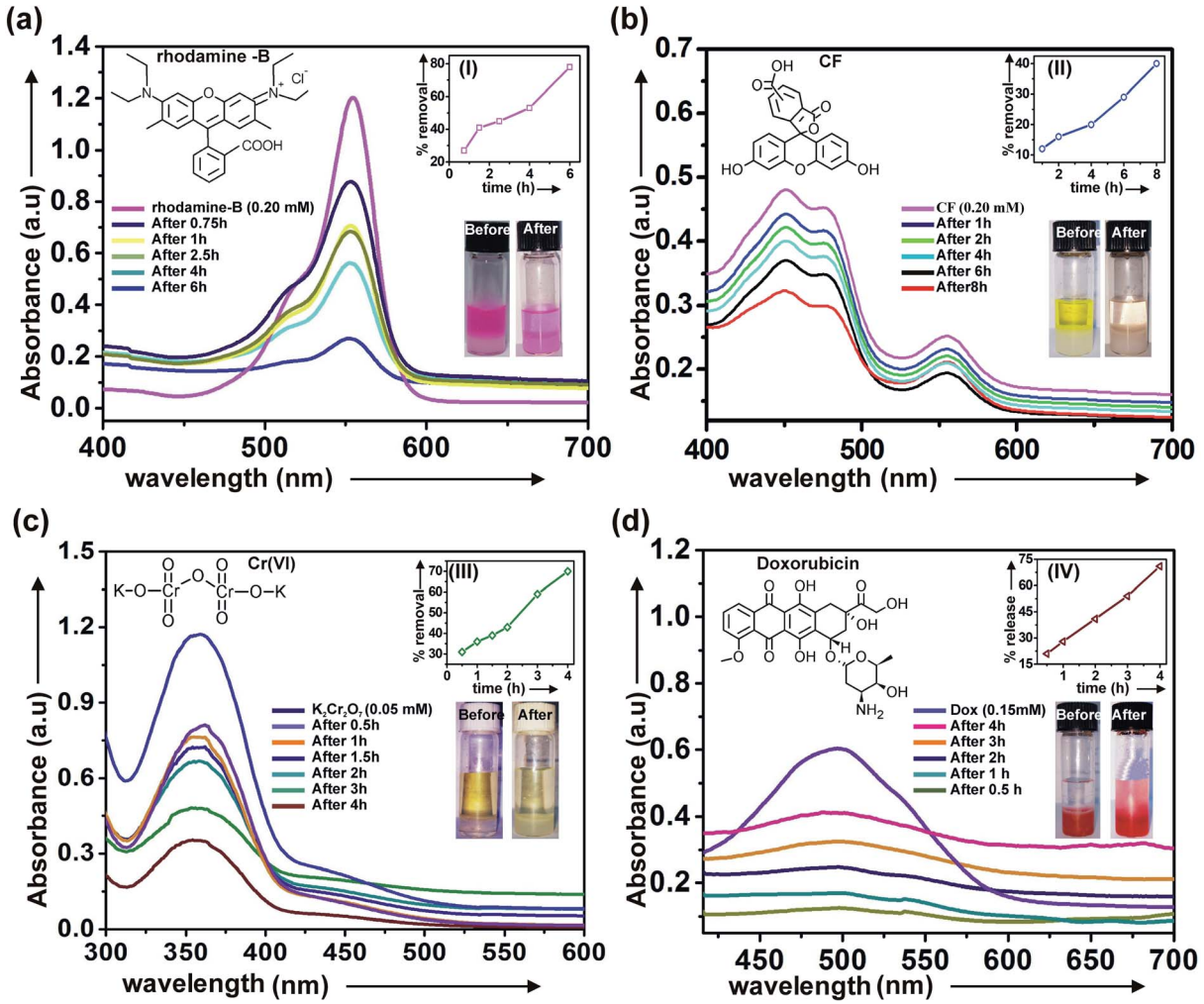

Fig. 11 Overlay of the UV-visible spectra for the removal of (a) rhodamine-B (0.20 mM) from its aqueous solution, (b) removal of CF (0.25 mM) from its aqueous solution at different time interval, (c) removal of Cr(VI) (0.05 mM) from its aqueous solution at different time interval, (d) overlay of the UV-visible spectra for the release of anticancer drug doxorubicin (0.15 mM) from loaded gel into PBS buffer at pH = 7.2 at different time interval; (I, II, III, IV) percentage of removal *vs.* time plot of rhodamine-B, CF, Cr(VI) and release of doxorubicin, inset: photographs of vials containing solutions of rho-B, CF, Cr(VI), Dox before and after the removal. The experiments were carried out at λ_{max} = 556 nm for rhodamine-B, λ_{max} = 456 nm for CF, λ_{max} = 372 nm for (Cr-VI) and λ_{max} = 520 nm for doxorubicin respectively.

indicated the release of drug in PBS buffer (Fig. 11d). Release of drug molecules into the buffer solution primarily took place *via* diffusion.[26] Spectral shape change observed with time indicated degradation of the gel. Traces of the presence of the anticancer drug doxorubicin still remaining inside the gels after 4 h of release (though less intense) was confirmed by epifluorescence microscopy carried out with the gel sample after the release experiment (Fig. S9, ESI†).

4 Conclusions

In conclusion, spontaneous formation of fibrillar self-assemblies of lupane-type mono-hydroxy terpenoid lupeol has been reported. According to our knowledge, this is the first report of the formation of self-assembled nano-fiber and sheets by naturally abundant 6–6–6–6–5 nano-sized mono-hydroxy terpenoid lupeol. A model for the self-assembly of lupeol have been proposed based on the morphology observed by AFM, optical, FESEM, HRTEM, concentration dependent FTIR studies, rheological studies and wide angle X-ray diffraction studies. The utilization of the gel of lupeol in DMSO–water for the removal of carcinogenic dyes like rho-B, CF including toxic heavy metal Cr(VI) from their respective aqueous solution has been demonstrated by UV-visible spectroscopic technique. Moreover, release of anti-cancer drug doxorubicin from drug loaded gel in PBS buffer at pH 7.2 has also been demonstrated by UV-visible spectroscopic technique.

5 Experimental

5.1 Materials

Lupeol was isolated from the dried and powdered outer bark of *Bombax ceiba* (yield = 0.2%) as a white solid. Solvents like *n*-heptane (Merck, SB9F690037), *n*-hexane (Merck, SI9F690620), *n*-ocatne (SDFCL, K09A/0409/2467/13), DMSO (Fischer Scientific, Lot No. 1910880417), DMF (SRL, 042825), cyclohexane (SRL, 6328103), THF (Merck, SK9SA91045), methanol (Rankem, KR110K17), *n*-butanol (Merck, SA6S550847), *n*-hexanol (SRL, 082795), ethanol (Rankem), *o*-dichlorobenzene (SRL, 04271), mesitylene (Loba Chemie, 0459700600), nitrobenzene (SRL, 75010), rho-B (SDFCL, K102/2210/140271), CF (Merck), Dox (Merck) were used in these studies.

5.2 Study of self-assembly and gelation

Lupeol (5 mg) was weighed in clean and dry vial (capacity = 4 mL). The compound was then mixed with a solvent and then heated (40–50 °C) for 20–25 min with magnetic stirring. Then the vial was kept at 15 °C under sealed condition for 2–8 h. Self-assembly was checked under optical microscopy. When the vial was turned upside down, no flow of solvents indicated the formation of a gel.

5.3 Preparation of gel for dye removal study

Lupeol (8 mg) was taken in a clean dried vial (capacity = 4 mL) was completely dissolved in distilled DMSO (0.6 mL) under heating condition with magnetic stirring, then distilled water (0.3 mL) was added dropwise to this solution. Thus the solution became cloudy which was redissolved by continuous heating and stirring magnetically. The resulting hot solution then allowed to cool at 15 °C. Opaqueness of the mixture inside the vial was observed for 2 h. No flow of the liquid by inverting the vial indicated the formation of a gel in DMSO–water (20.8 mM, 2 : 1 v/v).

5.4 Preparation of gel for rheological studies

Lupeol (6 mg) was dissolved in 200 mL of distilled DMSO under hot condition followed by magnetic stirring. Then distilled water (100 μL) was added dropwise into the hot solution and hence a cloudiness appeared which was further re-dissolved under hot condition followed by magnetic stirring and kept at 15 °C for 2–4 h. Thus, a gel of **1** in DMSO–H_2O (2 : 1 v/v, 2.0% w/v) was obtained. Similarly, compound **1** (8.5 mg) was dissolved in 225 mL of distilled DMSO under hot condition followed by magnetic stirring. Then distilled water (113 μL) was added dropwise into the hot solution and hence a cloudiness appeared which was further redissolved under hot condition followed by magnetic stirring and kept at 15 °C for 2–4 h. Thus a gel of **1** in DMSO–H_2O (2 : 1 v/v, 2.5% w/v) was obtained. Similarly another gel in DMSO–H_2O (2 : 1 v/v, 3.5% w/v) was also prepared. Following the similar procedure gels of **1** in DMF (at concentrations 2.0% w/v, 2.5% w/v and 3.5% w/v) were prepared. Following the similar procedure, gels of **1** in *n*-octane (at concentrations 2.0% w/v, 2.5% w/v and 3.5% w/v) were also prepared for rheological studies.

5.5 Preparation of doxorubicin loaded gel and study or drug release

Lupeol (8 mg) was dissolved in DMSO–water (2 mL, 3 : 2 v/v) under hot condition. Anticancer drug doxorubicin (0.5 mM, 100 μL) was added to the lupeol solution and heated with stirring to obtain a clear solution. The resulting solution was kept at 15 °C for 2–4 h and formation of a coloured gel loaded with doxorubicin (0.15 mM) was observed. Then 1.5 mL of PBS buffer solution (pH 7.2) was placed carefully on the top of the gel surface. Aliquots buffer layer (1.4 mL) was carefully collected at different time intervals and absorbance was measured at 520 nm. The absorbance values were plotted against time (Fig. 11d). Increase in the absorbance values with time indicated the release of drug in PBS buffer.

5.6 UV spectrophotometry

UV-1800 (SHIMADZU) UV-spectrophotometer was used for all the absorbance measurements. keeping wavelength (800–300 nm), scan speed = fast, slit width = 1 nm, scan mode = single. Quartz cuvette (capacity = 4 mL, l = 1 cm) was used for all the experiments. The absorption/release experiments were carried out at λ_{max} = 556 nm (rho-B), λ_{max} = 456 nm (CF), λ_{max} = 372 nm (Cr-VI) and λ_{max} = 520 nm (doxorubicin) respectively.

5.7 FTIR

FTIR spectra of all the samples were recorded in PerkinElmer FTIR C98747 Instrument in the range 4000–400 cm^{-1}, resolution = 4 cm^{-1}, data interval = 1 cm^{-1}, accumulation = 4 scans.

5.8 Rheology

A modular compact rheometer (Anton Paar model MCR102) with a plate–plate assembly equipped with a temperature control system where the upper plate had a diameter of 25 mm (PP25) was used for all rheological measurements. All the rheology experiments were performed at temperature = 25 °C, at LVER default mode, shear strain (γ, %) = 0.01–100, angular frequency (ω) = constant at 10 (1 s^{-1}), oscillatory stress = 0.001–100 Pa, frequency = 10 S^{-1}, gap (d) = 0.105 mm, sensor force (F_s) = −0.03 to −0.05 N, data point number = 25.

5.9 Epifluorescence microscopy

Epifluorescence microscopy was carried out in Carl Zeiss microscope: Axio scope A1 attached with a fluorescence light source. For these experiments the coloured gels after the removal/release experiments were collected carefully and placed on glass slide and covered with cover slip and observed under epifluorescence microscope.

Conflicts of interest

The authors declare no conflict of interest.

Acknowledgements

BGB thanks Indo Sri Lanka project (DST/INT/SL/P25/2016), CSIR, UGC-SAP and DST-FIST New Delhi and Vidyasagar University for financial support and infrastructural facilities. SKP acknowledge UGC BSR for research fellowships.

Notes and references

1 K. Ohyamaa, M. Suzukia, J. Kikuchi, K. Saitoa and T. Muranakaa, *Proc. Natl. Acad. Sci. U. S. A.*, 2009, **106**, 725.
2 E. J. Corey, S. P. T. Matsuda and B. Bartel, *Proc. Natl. Acad. Sci. U. S. A.*, 1993, **90**, 11628.
3 B. Kamm, *Angew. Chem., Int. Ed.*, 2007, **46**, 5056.
4 A. Gandini, *Green Chem.*, 2011, **13**, 1061.
5 B. G. Bag, A. C. Barai, S. N. Hasan, S. K. Panja, S. Ghorai and S. Patra, *Pure Appl. Chem.*, 2019, **92**, 567.
6 M. George and R. G. Weiss, *Acc. Chem. Res.*, 2006, **39**, 489.
7 B. G. Bag and R. Majumdar, *Chem. Rec.*, 2017, **17**, 841.
8 E. Carretti, M. Bonini, L. Dei, B. H. Berrie, L. V. Angelova, P. Baglioni and R. G. Weiss, *Acc. Chem. Res.*, 2010, **43**, 751–760.
9 S. Bhattacharya and S. K. Samanta, *Chem. Rev.*, 2016, **116**, 11967.
10 K. Hanabusa, *Springer Ser. Mater. Sci.*, 2004, **78**, 118.
11 *Molecular Gels: Materials with Self-Assembled Fibrillar Networks*, ed. R. G. Weiss and P. Terech, Springer, 2006.
12 E. Carretti, M. Bonini, L. Dei, B. H. Berrie, L. V. Angelova, P. Baglioni and R. G. Weiss, *Acc. Chem. Res.*, 2010, **43**, 751.
13 M. de Loos, B. L. Feringa and J. H. van Esch, *Eur. J. Org. Chem.*, 2005, 3615.
14 S. K. Panja and B. G. Bag, *ACS Omega*, 2020, **5**, 30488.
15 S. Ghorai and B. G. Bag, *ACS Omega*, 2021, **6**, 20560.
16 A. Vintilou and J. C. Leroux, *J. Controlled Release*, 2008, **125**, 179.
17 J. H. Jung and S. Shinkai, *Top. Curr. Chem.*, 2004, **248**, 223.
18 R. V. Ulijn and A. M. Smith, *Chem. Soc. Rev.*, 2008, **37**, 664.
19 M. O. M. Piepenbrock, G. O. Lloyd, N. Clarke and J. W. Steed, *Chem. Rev.*, 2010, **110**, 1960.
20 T. Kato, *Science*, 2002, **295**, 2414.
21 J. P. Luis, V. Laukhin, A. P. del Pino, J. V. Gancedo, C. Rovira, E. Laukhina and D. B. Amabilino, *Angew. Chem., Int. Ed.*, 2007, **46**, 238.
22 W. Kubo, S. Kambe, S. Nakade, T. Kitamura, K. Hanabusa, Y. Wada and S. Yanagida, *J. Phys. Chem. B*, 2003, **107**, 4374.
23 S. Li, V. T. John, G. C. Irvin, S. H. Bachakonda, G. L. McPherson and C. J. O'Connor, *J. Appl. Phys.*, 1999, **85**, 5965.
24 D. D. Diaz, D. Kuhbeck and R. J. Koopmans, *Chem. Soc. Rev.*, 2011, **40**, 427.
25 B. G. Bag, G. C. Maity and S. K. Dinda, *Org. Lett.*, 2006, **8**, 5457.
26 B. Mondal, D. Bairagi, N. Nandi, B. Hansda, K. S. Das, C. J. C. E. Gayle, V. Castelletto, I. W. Hamley and A. Banerjee, *Langmuir*, 2020, **36**, 12942.
27 K. Basu, N. Nandi, B. Mondal, A. Dehsorkhi, I. W. Hamley and A. Banerjee, *Interface Focus*, 2017, **7**, 20160128.
28 L. A. Estroff and A. D. Hamilton, *Chem. Rev.*, 2004, **104**, 1201.
29 P. Xie and R. Zhang, *J. Mater. Chem.*, 2005, **15**, 2529.
30 A. Ajayaghosh, V. K. Praveen and C. Vijayakumar, *Chem. Soc. Rev.*, 2008, **37**, 109.
31 D. K. Smith, *Chem. Commun.*, 2006, 34–44.
32 M. Delample, F. Jerome, J. Barrault and J. P. Douliez, *Green Chem.*, 2011, **13**, 64.
33 B. Novales, L. Navailles, M. Axelos, F. Nallet and J. P. Douliez, *Langmuir*, 2008, **24**, 62.
34 J. P. Douliez, *J. Am. Chem. Soc.*, 2005, **127**, 15694.
35 N. Baccile, N. Nassif, L. Malfatti, I. N. A. VanBogaert, W. Soetaert, G. P. Arnaudet and F. Babonneau, *Green Chem.*, 2010, **12**, 1564.
36 S. Zhou, C. Xu, J. Wang, W. Gao, R. Khverdiyeva, V. Shah and R. Gross, *Langmuir*, 2004, **20**, 7926.
37 Y. Jang and J. A. Champion, *Acc. Chem. Res.*, 2016, **49**, 2188.
38 D. Das, T. Kar and P. K. Das, *Soft Matter*, 2012, **8**, 2348.
39 P. Koley and A. Pramanik, *Adv. Funct. Mater.*, 2011, **21**, 4126.
40 S. Datta and S. Bhattacharya, *Chem. Soc. Rev.*, 2015, **44**, 5596.
41 H. Kobayashi, A. Friggeri, K. Koumoto, M. Amaike, S. Shinkai and D. N. Reinhoudt, *Org. Lett.*, 2002, **4**, 1423.
42 E. Virtane and E. Kolehmainen, *Eur. J. Org. Chem.*, 2004, **16**, 3385.
43 N. He, K. Zhi, X. Yang, H. Zhao, H. Zhang, J. Wang and Z. Wang, *New J. Chem.*, 2018, **42**, 14170.
44 B. G. Bag and S. S. Dash, *Nanoscale*, 2011, **3**, 4564.
45 B. G. Bag, S. N. Hasan, P. Pongpamorn and N. Thasana, *ChemistrySelect*, 2017, **2**, 6650.
46 F. O. deLima, V. Alves, J. M. B. Filho, J. R. G. da Silva Almeida, L. C. Rodrigues, M. B. P. Soares and C. F. Villarreal, *Phytother. Res.*, 2013, **27**, 1557–1563.
47 M. Saleem, *Cancer Lett.*, 2009, **285**, 109.

48 D. Palanimuthu, N. Baskaran, S. Silvan, D. Rajasekaran and S. Manoharan, *Pathol. Oncol. Res.*, 2012, **18**, 1029.
49 R. K. Ambasta, S. K. Jha, D. Kumar, R. Sharma, N. K. Jha and P. Kumar, *J. Transl. Med.*, 2015, **13**, 307.
50 T. O. Vieira, A. Said, E. Aboutabl, M. Azzam and T. B. C. Pasa, *Redox Rep.*, 2009, **14**, 41.
51 K. Hata, S. Ogawa, M. Makino, T. Mukaiyama, K. Hori, T. Iida and Y. Fujimoto, *J. Nat. Med.*, 2008, **62**, 332.
52 H. H. Kwon, J. Y. Yoon, S. Y. Park, S. Min, Y. Kim, J. Y. Park, Y. S. Lee, D. M. Thiboutot and D. H. Suh, *J. Invest. Dermatol.*, 2015, **135**, 1491.
53 P. T. Sudharsan, Y. Mythili, E. Selvakumar and P. Varalakshmi, *Mol. Cell. Biochem.*, 2006, **282**, 23.
54 S. K. Panja and B. G. Bag, *Prayogik Rasayan*, 2019, **3**, DOI: 10.53023/p.rasayan-20191212.
55 K. Zhi, H. Zhao, X. Yang, H. Zhang, J. Wang and Z. Wang, *ChemPlusChem*, 2018, **83**, 797.
56 P. Terech, D. Pasquier, V. Bordas and C. Rossat, *Langmuir*, 2000, **16**, 4485.
57 J. Brinksma, B. L. Feringa, R. M. Kellogg, R. Vreeker and J. V. Esch, *Langmuir*, 2000, **16**, 9249.
58 K. Lalitha, a. Y. Siva Prasad, V. Sridharan, C. U. Maheswari, G. John and S. Nagarajan, *RSC Adv.*, 2015, **5**, 77589.
59 B. G. Bag, S. Ghorai, S. K. Panja, S. K. Dinda and K. Paul, *RSC Adv.*, 2018, **8**, 29155.
60 A. Dawn and H. Kumari, *Chem.–Eur. J.*, 2018, **24**, 762.
61 M. J. Kamlet, J. L. M. Abboud, M. H. Abraham and R. W. Taft, *J. Org. Chem.*, 1983, **48**, 2877.
62 A. R. Hirst and D. K. Smith, *Langmuir*, 2004, **20**, 10851.
63 J. Fredericks, J. Yang, S. J. Geib and A. D. Hamilton, *Proc. - Indian Acad. Sci., Chem. Sci.*, 1994, **106**(5), 923.
64 S. Manchineella and T. Govindaraju, *RSC Adv.*, 2012, **2**, 5539.
65 H. Kar, D. Gehrig, F. Laquai and S. Ghosh, *Nanoscale*, 2015, **7**, 6729–6736.
66 X. Cao, N. Zhao, R. Li, H. Lv, Z. Zhang, A. Gao and T. Yi, *Chem.–Asian J.*, 2016, **11**, 3196.
67 N. T. Nguyen and J. H. Liu, *Sci. Adv. Mater.*, 2015, **7**, 1282.
68 R. S. Corre, C. P. Coelho, M. H. D. Santos, J. Ellenaa and A. C. Doriguettoc, *Acta Crystallogr., Sect. A: Found. Adv.*, 2009, **65**, 97.
69 B. G. Bag and A. C. Barai, *RSC Adv.*, 2020, **10**, 4755.